A novel transparent metasurface for polarization-reconfigurable vortex wave generation

A novel transparent metasurface for polarization-reconfigurable vortex wave generation

K Y Liu, G M Wang[1] and W L Guo

Air and Missile Defense College, Air Force Engineering University, Xi'an 710051, People's Republic of China

[1] E-mail: wgming01@sina.com

Abstract. Since the orbital angular monument (OAM) can improve the channel capability enormously, the generation of vortex wave carrying OAM has became research hotspots. In this paper, a novel metasurface is proposed which can generate vortex wave in arbitrary polarization states. By varying the polarization direction of the incident wave, the polarization of the vortex wave switch between linear polarization, elliptical polarization and circular polarization. The simulation results verify that the metasurface can generate vortex wave in x-pol, right hand circular polarization, y-pol and left hand circular polarization in 14GHz. The proposed method can pave the way to generate vortex wave in wireless communication applications.

1. Introduction

In recent decades, information is generally transmitted through wireless channels and the rapid growth of mobile devices has led to congestion in the available radio spectrum even after the application of information processing techniques such as dense coding and channel sharing. Consequently, exploiting the physical properties of the electromagnetic (EM) wave that hitherto have not been used in wireless communication, is of great importance to improve the channel capacity. According to the EM theory, EM wave not only carries linear momentum but carry angular momentum [1]. Linear momentum is related to the Poynting vector, and the angular momentum consists of spin angular momentum (SAM) [2] and orbital angular momentum (OAM) [3]. The SAM depicts the polarization states of EM waves while OAM is associated with the twist of a spiral phase wavefront. Since different eigenstates of OAM are orthogonal to each other, they can offer an additional degree of freedom. Thanks to the OAM features, the spatially orthogonal overlapping and co-propagating OAM modes can be utilized as an approach of enhancing data capacity and eliminating limitation of communication systems without increasing the frequency bandwidth. In 2007, Thidé performed the first radio OAM simulation by phased array antenna, which has produced vortex wave in radio frequency domain [4]. In 2012, Fabrizio Tamburini firstly transmit two independent radio channels simultaneously in two different OAM states in a real-world setting, which demonstrates that OAM states can dramatically enhance the channel capacity in any spectrums [5].

To date, various methods are proposed to generate radio and optical vortices, such as spiral phase plates [6-7], spiral reflectors [4, 8], holographic diffraction gratings [9-10], antenna arrays [11-12]. Metasurface (MS), as a 2D version of metametrial has unprecedented capability of manipulating EM wave-fronts and is widely utilized to generate vortex wave. By exploiting Pancharatnam-Berry phase concept and anisotropic scatters, reflective and broadband MS are synthesized to create single and

multiple vortex beam carrying OAM [13-17]. However, these works are usually restricted to generate vortex wave in a fixed polarization states. In this paper, we propose a strategy to design a novel MS which can generate vortex wave in arbitrary polarization. The MS composed of 19×19 elements with special phase profile are engineered and simulated. By controlling the polarization direction of the incident wave, the polarization states of the vortex wave will be manipulated. The simulation results show that the novel MS creates OAM carrying vortex wave in x-pol, right hand circular polarization (RHCP), y-pol and left hand circular polarization (LHCP). This work provides an approach to manipulating the polarization state of vortex beam in microwave wireless applications.

2. Theoretical analysis and design

2.1. Theoretical analysis

The phase distribution of the MS is composed of hyperbolical phase distribution and spiral phase distribution. The former one is to generate plane wave and the later one is to introduce azimuthal phase dependence. Patch antenna is usually selected as the feed source, so the hyperbolical phase distribution should be introduced to transform the quasi-spherical wave into plane wave. The hyperbolical phase distribution can be expressed as:

$$\phi_{foc}(m,n) = k(\sqrt{F^2 + (mp)^2 + (np)^2} - F) \tag{1}$$

Where F is the focal length, p is the periodicity of the element, and $\phi_{foc}(m,n)$ is depicted in Figure 1(a). Based on plane wave, the key factor to generate vortex wave is to introduce azimuthal phase dependence $e^{-jl\varphi}$ into the wave, so the phase distribution should obey the following formula:

$$\phi_{vor}(m,n) = l\varphi = l\tan^{-1}\left(\frac{n}{m}\right) \tag{2}$$

Where the l is the topological charge of OAM mode, φ is the azimuthal angle, m and n represent the number of elements in the x and y directions and $\phi_{\mathrm{vor}}(m,n)$ is plotted in Figure 1(b). Thus, the phase distribution is the combination of $\phi_{foc}(m,n)$ and $\phi_{\mathrm{vor}}(m,n)$ as depicted in Figure 1(c), following the formula:

$$\begin{aligned}\phi(m,n) &= \phi_{foc}(m,n) + \phi_{vor}(m,n) \\ &= l\tan^{-1}(\frac{n}{m}) + k(\sqrt{F^2 + (mp)^2 + (np)^2} - F)\end{aligned} \tag{3}$$

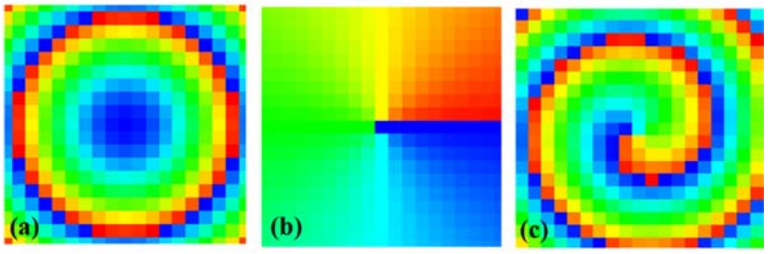

Figure 1. The phase distribution of (a) $\phi_{foc}(m,n)$, (b) $\phi_{\mathrm{vor}}(m,n)$, (c) $\phi(m,n)$.

Next the we describe the theory of polarization conversion. Assuming a beam of EM wave is propagating along the +z direction, the electric field of incident wave can be described as

$$\boldsymbol{E}_i = (\boldsymbol{a}_x E_x + \boldsymbol{a}_y E_y) \tag{4.a}$$

$$\begin{pmatrix} E_x \\ E_y \end{pmatrix} = \begin{pmatrix} \cos\alpha \\ \sin\alpha \end{pmatrix} e^{-jkz} \tag{4.b}$$

Where $\boldsymbol{a}_x$ and $\boldsymbol{a}_y$ is the unit vectors in x and y direction, E_x and E_y represent the x-polarized and y-polarized component, $k=\frac{2\pi}{\lambda}$ is propagation constant, α is the angle between E and +x-axis. The transmitted electric field through the MS is

$$\boldsymbol{E}_t = (\boldsymbol{a}_x E_x' + \boldsymbol{a}_y E_y') \tag{5.a}$$

$$\begin{pmatrix} E_x' \\ E_y' \end{pmatrix} = \boldsymbol{T}\begin{pmatrix} E_x \\ E_y \end{pmatrix} = \begin{pmatrix} T_{xx} & T_{xy} \\ T_{yx} & T_{yy} \end{pmatrix}\begin{pmatrix} \cos\alpha \\ \sin\alpha \end{pmatrix} e^{-jkz} \tag{5.b}$$

Where E_x' and E_y' represent the x-polarized and y-polarized component of transmitted E field, $\boldsymbol{T}$ is the transmission matrix. To get circular polarized wave, the transmission coefficient should meet the following conditions that $\left|\text{phase}(T_{xx})-\text{phase}(T_{yy})\right|=\frac{\pi}{2}$, $\left|T_{xx}\right|=\left|T_{yy}\right|=1$ and T_{xy}=T_{yx}=0. The transmitted matrix can be described as

$$T=\begin{pmatrix} -j & 0 \\ 0 & 1 \end{pmatrix} e^{-j\phi} \tag{6}$$

Thus, there should have 90° phase difference between the phase distribution for x-pol and y-pol as depicted in for Eq. (7).

$$\phi_{x-pol}(m,n)=\phi_{foc}(m,n)+\phi_{vor}(m,n) \tag{7.a}$$

$$\phi_{y-pol}(m,n)=\phi_{foc}(m,n)+\phi_{vor}(m,n)+\frac{\pi}{2} \tag{7.b}$$

With ϕ=ϕ_{vor}+ϕ_{foc} obtained from MS, in the case of α=0°, 45°, 90° and 135°， the transmitted E fields can be calculated as

$$\boldsymbol{E}_t^{0} = -j\boldsymbol{a}_x e^{-jkz} e^{-j\phi_{foc}} e^{-jl\varphi} \tag{8}$$

$$\boldsymbol{E}_t^{45} = \frac{1}{\sqrt{2}}(-j\boldsymbol{a}_x+\boldsymbol{a}_y) e^{-jkz} e^{-j\phi_{foc}} e^{-jl\varphi} \tag{9}$$

$$\boldsymbol{E}_t^{90} = \boldsymbol{a}_y e^{-jkz} e^{-j\phi_{foc}} e^{-jl\varphi} \tag{10}$$

$$\boldsymbol{E}_t^{135} = \frac{1}{\sqrt{2}}(-j\boldsymbol{a}_x+\boldsymbol{a}_y) e^{-jkz} e^{-j\phi_{foc}} e^{-jl\varphi} \tag{11}$$

It is obvious that the hyperbolical phase shift $e^{-j\phi_{foc}}$ and azimuthal phase dependence $e^{-jl\varphi}$ are introduced into the transmitted wave, thus the spherical wavefront will be transformed into spiral wavefront. When α=45° and 135°, the vortex waves are in LHCP and RHCP which are different from the linear polarization of the incident wave. In the case of α=0°and α=90°, the incident wave only contains *x*-polarized wave or *y*-polarized wave, and the transmitted wave will be reduced to linearly polarized vortex wave.

2.2. MS design

To begin with, an anisotropic rectangular patch is selected as the meta-atom of the MS. As shown in Figure 2(a), the anisotropic element is composed of four metallic patch layers and three intermediate dielectric layers. Each metallic layer contains the same rectangular patch, and dielectric layer has a permittivity of ε_r=4.3 and thickness of h=1 mm. As depicted in Figure 2(b), the element is illuminated by a plane wave propagating along +z direction with unit cell boundaries applied in the x and y directions, and open boundaries applied in z direction. The 2D map of amplitude and phase shift of T_{yy} versus Px and Py are depicted in Figure 2(c), (d), where the phase shift coverage over 360° and transmissivity $|T_{yy}|$ is greater than 0.72. When Px is fixed as 3, the phase shift changes from -330°to 40 by varying Py from

4.67mm to 2mm. The simulation phase shift verifies that the element possesses independent control of x- and y-polarization.

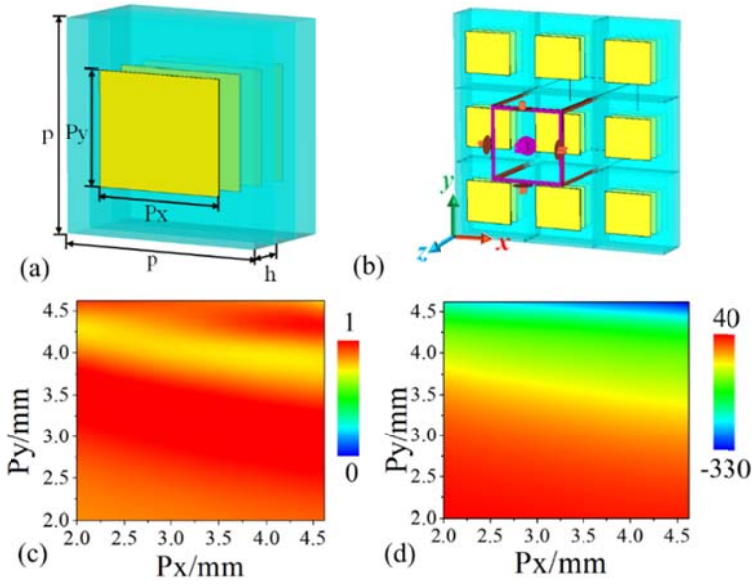

Figure 2. Design and simulation of the element. The (a) prototype of the unit cell where p = 6.8 mm and the (b) perspective view of the simulation setup. The 2D map of the (c) amplitude and (d) transmission phase shift of T_{yy}.

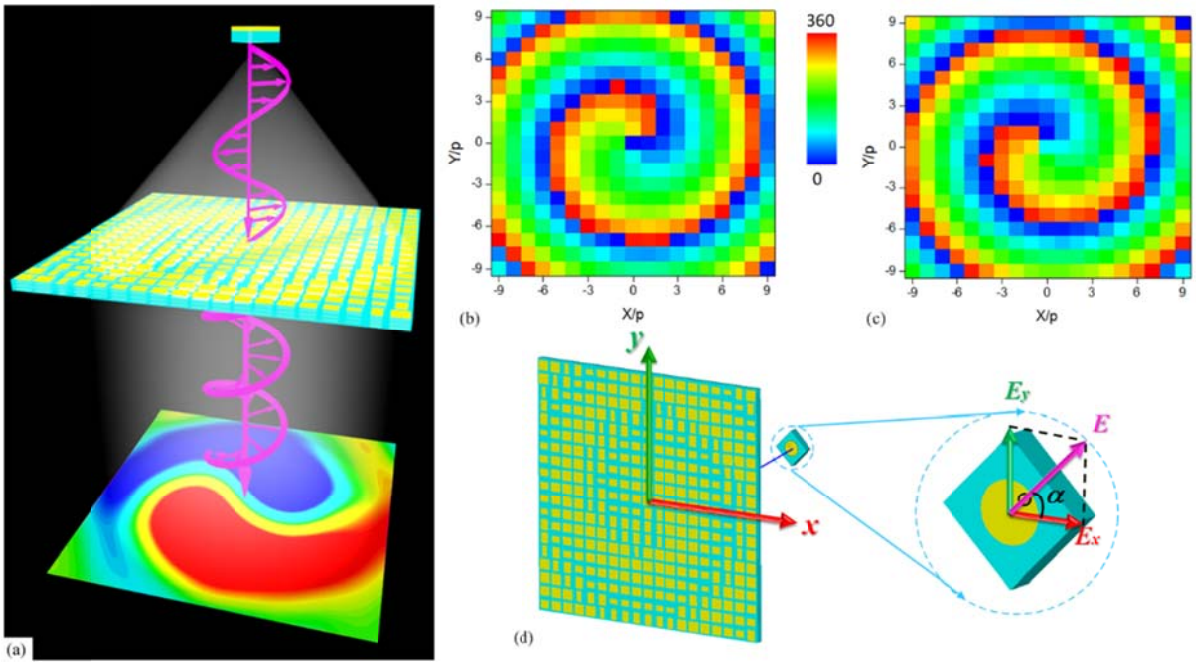

Figure 3. (a)Working principle of the MS. Transmission phase distributions for (b) x-polarized and (c) y-polarized wave. (d) Geometry implementation of the MS based on rectangular patch element. The magnified insert view depicts the patch antenna with rotation angle of α.

Based on the element, we propose a MS with size of 149.6 × 149.6 mm^2 and elements of 22 × 22 with operating phenomenon shown in Figure 3(a). As seen, a beam of vortex RHCP wave is easily achieved just through a compact ultra-thin MS, which may provide a promising approach to design

multi-functional vortex beam generators. The phase distribution for x-pol and y-pol are shown in Figure 3 (b), Figure 3 (c). Notably, a patch antenna with a tunable rotation angle as shown in Figure 3(d) is employed to radiate differently linear polarization wave, so as to achieve vortex beams operating in differently polarized modes.

3. Simulation results

To illustrate the operating performance of the MS, the full-wave electromagnetic simulation was carried out in CST Microwave Studio. With open boundary conditions applied in all directions, the vortex generator is simulated with incident wave under the case of α 0°, 45°, 90° and 135°. The E-field distributions and far-field results of the MS under the illumination of linearly polarized wave with are simulated. The real parts of the E field and the phase distribution presented in Figure 4 (a), (d), (g), (j) reveal that OAM vortex wave is generated by employing the proposed MS. It is apparent that spiral phase distribution is obtained and there is a phase singularity whose energy is zero locates at the center of the near field zone. As depicted in far field radiation pattern, there is a wave valley in the direction of main lobe. What's more, according to the preceding theoretical analysis, when α=45° and 135°, the transmitted wave will be in LHCP and RHCP. And in the special case of α=0° and α=90°, the transmitted wave is reduced into linearly polarized vortex wave. To verity the circular polarization of the vortex wave in the case of α=45° and α=135°, the axis ratios in xoz φ= 90° and yoz φ = 0°plane are plotted in Figure 5. It is clearly that the axis ratio is lower than 3dB near the range of θ = 10°.

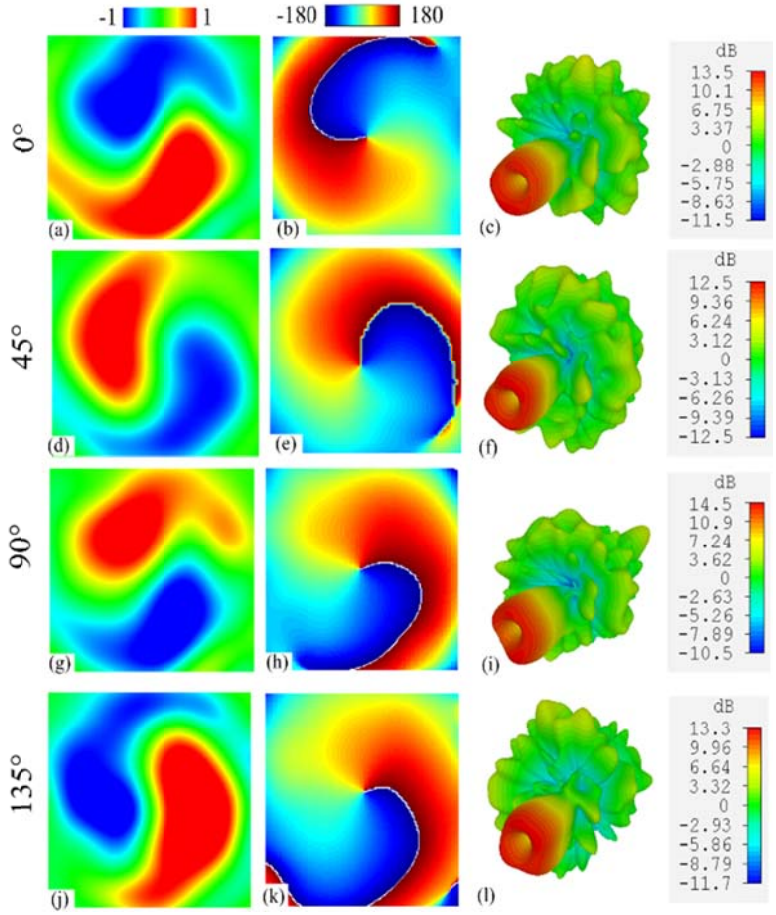

Figure 4. Simulated near field and far-field results of MS. (a), (d), (g), (j) are Re(E) of transmitted wave. (b), (e), (h), (k) are phase distributions of E field. (c), (f), (i), (l) are 3d far-field radiation patterns. The first, second, third and fourth row represent the simulated results in the case of α=0°, α=45°, α=90° and α=135°.

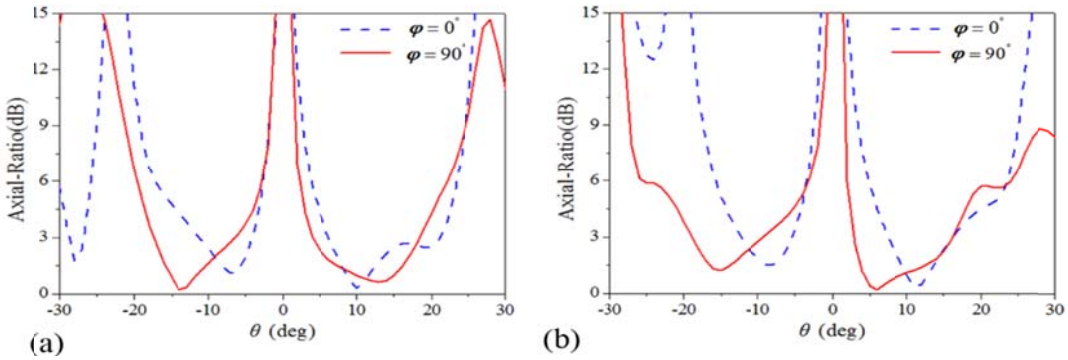

Figure 5. Simulated axis ratio of the circularly polarized vortex wave in the case of (a) α=0°, (b) α=45°.

4. Conclusions

To sum up, a novel transparent MS for polarization-reconfigurable vortex wave generation is designed and simulated. Based on anisotropic unit cell, the MS can not only generate vortex phase wavefront, but can manipulate the polarization states of the vortex wave. When the incident wave contains both two orthogonal linear polarization components, the transmitted vortex wave will be in circular polarization. And when the incident wave only contains one orthogonal linear polarization component, the transmitted wave has deduced into linearly polarized vortex waves. According to the simulated results, vortex wave with four kinds of polarization states (RHCP, LHCP, x-polarized, y-polarized) can be produced with spiral wave-fronts. What's more, measurement will be carried out to verify the performance of the MS in the next step. The vortices of OAM beams contain a theoretically unlimited range of possibly eigenstates which offer an additional degree of freedom and is promising in improving capability of communication channels. This work is free of complex network and may pave way to a new paradigm in radio wireless communication.

References

[1] J Zhou, Zhang W H and Chen L X 2016 *Appl. Phys. Lett.* **108** 111108
[2] T Omatsu, K Chujo, K Miyamoto, M Okida, K. Nakamura, N Aoki and R Morita 2010 *Opt. Express* **18** 17967
[3] X Gao, S Huang, Y Wei, W Zhai, W Xu, S Yin, J Zhou and W Gu 2014 *Appl. Phys. Lett.* **105** 241109
[4] B Thidé, H Then, J Sj€oholm, K Palmer et al. 2007 *Rev. Lett.* **99** 087701
[5] F Tamburini, E Mari, A Sponselli, B Thidé et al. 2012 *New J. Phys.* **14** 033001
[6] M Uchida and A Tonomura 2010 *Nature* **464** 7289
[7] L Cheng, W Hong, and Z C Hao 2014 *J. Sci. Rep.* **4** 4814
[8] X Hui, S Zheng, Y Hu, C Xu, X Jin, H Chi, X Zhang 2015 *IEEE Antennas Wireless Propag. Lett.* **14** 966
[9] S Chavez-Cerda, M J Padgett, I Allison, G H C New, J C Gutierrez-Vega, A T O'Neil, I Macvicar and J Courtial 2002 *Opt. B: Quantum Semiclassical Opt*. **4** S52
[10] F Capasso, P Genevet, J Lin and M A Kats 2012 *Nature Comm*. **3** 1278
[11] S M Mohammadi, L K S Daldorff, J E S Bergman and R L Karlsson 2010 *IEEE Trans. Antennas Propag.* **58** 565
[12] X Y Lei and Y J Cheng 2017 *IEEE Antennas Wireless Propag. Lett.* **16**
[13] K Zhang, Y Yuan, D Zhang, X Ding, BRatni, S NBurokur, M Lu, KTang, Q Wu 2018 *OPTICS EXPRESS* **26** 1353
[14] M Q Mehmood, Shengtao Mei , Sajid Hussain , Kun Huang, S Y Siew, L Zhang, TZhang, X Ling , H Liu, J Teng, A Danner, S Zhang and C-W Qiu 2016 *Adv. Mater.* **28** 2533

[15] S X Yu, L Li, G M Shi, C Zhu, X X Zhou and Y Shi 2016 *Appl. Phys. Lett.* **108** 121903
[16] S X Yu, L Li, G M Shi, C Zhu and Y Shi 2016 *Appl. Phys. Lett.* **108** 241901
[17] H X Xu, H W Liu, X H, Ling, Y M Sun and F Yuan 2017 *IEEE Trans. Antennas Propag*. **12** 65